Atmospheric Environment 44 (2010) 3568–3582

Contents lists available at ScienceDirect

Atmospheric Environment

journal homepage: www.elsevier.com/locate/atmosenv

Simulating chemistry–aerosol–cloud–radiation–climate feedbacks over the continental U.S. using the online-coupled Weather Research Forecasting Model with chemistry (WRF/Chem)

Yang Zhang [a,*], X.-Y. Wen [a], C.J. Jang [b]

[a] Department of Marine, Earth, and Atmospheric Science, North Carolina State University, Campus Box 8208, Raleigh, NC 27695, USA
[b] Office of Air Quality Planning and Standards, US Environmental Protection Agency, Research Triangle Park, NC 27711, USA

ARTICLE INFO

Article history:
Received 12 February 2010
Received in revised form
27 May 2010
Accepted 31 May 2010

Keywords:
WRF/Chem
Aerosol direct effects
Aerosol indirect effects
CCN
Cloud droplet number concentrations

ABSTRACT

The chemistry–aerosol–cloud–radiation–climate feedbacks are simulated using WRF/Chem over the continental U.S. in January and July 2001. Aerosols can reduce incoming solar radiation by up to −9% in January and −16% in July and 2-m temperatures by up to 0.16 °C in January and 0.37 °C in July over most of the continental U.S. The NO_2 photolysis rates decrease in July by up to −8% over the central and eastern U.S. where aerosol concentrations are high but increase by up to 7% over the western U.S. in July and up to 13% over the entire domain in January. Planetary boundary layer (PBL) height reduces by up to −23% in January and −24% in July. Temperatures and wind speeds in July in big cities such as Atlanta and New York City reduce at/near surface but increase at higher altitudes. The changes in PBL height, temperatures, and wind speed indicate a more stable atmospheric stability of the PBL and further exacerbate air pollution over areas where air pollution is already severe. Aerosols can increase cloud optical depths in big cities in July, and can lead to 500–5000 cm^{-3} cloud condensation nuclei (CCN) at a supersaturation of 1% over most land areas and 10–500 cm^{-3} CCN over ocean in both months with higher values over most areas in July than in January, particularly in the eastern U.S. The total column cloud droplet number concentrations are up to 4.9×10^6 cm^{-2} in January and up to 11.8×10^6 cm^{-2} in July, with higher values over regions with high CCN concentrations and sufficient cloud coverage. Aerosols can reduce daily precipitation by up to 1.1 mm day^{-1} in January and 19.4 mm day^{-1} in July thus the wet removal rates over most of the land areas due to the formation of small CCNs, but they can increase precipitation over regions with the formation of large/giant CCN. These results indicate potential importance of the aerosol feedbacks and an urgent need for their accurate representations in current atmospheric models to reduce uncertainties associated with climate change predictions.

© 2010 Elsevier Ltd. All rights reserved.

1. Introduction

The complex feedback mechanisms among chemistry–aerosol–cloud–radiation–climate exist ubiquitously in the Earth systems and represent one of the most uncertain research areas in understanding climate change and its potential impact on atmosphere (Jacobson, 2002; IPCC, 2007; Zhang, 2008; Jacob and Winner, 2009). The feedbacks of aerosols may include a reduction of downward solar radiation (direct effect); a decrease in surface/near surface temperature and wind speed, as well as planetary boundary layer (PBL) height but an increase in relative humidity (RH) and atmospheric stability (semi-direct effect), a decrease in cloud drop size but an increase in cloud droplet number concentrations (CDNC) via serving as cloud condensation nuclei (CCN) (first indirect effect or cloud albedo effect), as well as an increase in liquid water content, cloud coverage, and lifetime of low-level clouds and either suppression or enhancement of precipitation (the second indirect effect or cloud lifetime effect). These feedbacks have been observed in numerous field experiments or through analyses of long-term historic surface and satellite observational data. For example, smoke from rain forest fires over Amazon and Indonesia and burning of agricultural vegetations can inhibit rainfall by shutting off warm rain-forming processes over these regions (Warner, 1968; Kaufman and Fraser, 1997; Rosenfeld and Lensky, 1998; Rosenfeld, 1999; Rosenfeld and Woodley, 1999). The suppression in orographic precipitation by anthropogenic aerosols was found to be 15–25% of the annual precipitation in hilly areas in California and Israel (Givati and Rosenfeld, 2004, 2005; Rosenfeld

* Corresponding author.
E-mail address: yang_zhang@ncsu.edu (Y. Zhang).

1352-2310/$ – see front matter © 2010 Elsevier Ltd. All rights reserved.
doi:10.1016/j.atmosenv.2010.05.056

et al., 2008a). The orographic precipitation observed at Mt. Hua near Xi'an in China decreased by 30–50% during hazy conditions in the presence of high levels of aerosols and small CCN based on the analyses of more than 50-year observations (Rosenfeld et al., 2007a). Enhanced rainfall, on the other hand, was found in (Braham et al., 1981; Cerveny and Bailing, 1998) and downwind (Eagen et al., 1974; Jauregui and Romales, 1996) of major urban areas and paper mills, suggesting that giant CCN can enhance precipitation. The two opposite effects of aerosols on precipitation are results of different aerosol radiative properties and CCN potentials under different conditions (Rosenfeld et al., 2008b). For example, atmospheric aerosols decrease net downward solar radiation reaching surface, causing less heat available for water evaporation thus suppressing precipitation. On the other hand, the strongly-absorbing aerosols such as mineral dust and particles from heavy smoke have been found to invigorate and restructure convective clouds due to the solar heating and induced convection by these aerosols (Levin et al., 1996, 2005; Rudich et al., 2003; Miller et al., 2004; Koren et al., 2005; Klüser et al., 2008; Levin and Brenguier, 2009), thus enhancing precipitation.Aerosols such as mineral dust and black carbon can also alter atmospheric circulation (e.g., Zanis, 2009) through changing the atmospheric heating and stability to affect the monsoons (Lau et al., 2006; Lau and Kim, 2006) and severe storms (Rosenfeld, 2006; Zhang et al., 2007; Bell et al., 2008; Ramanathan and Carmichael, 2008 and references therein).

Accurately simulating these feedbacks requires the use of online-coupled meteorology-chemistry models; among which the NOAA Weather Research and Forecasting Model with Chemistry (WRF/Chem) of Grell et al. (2005) represents a state-of-the-science online model. While most air quality modeling has focused on accessing the models' capability in capturing past pollution episodes and forecasting short-term (2–4 days) air quality, there have been fewer studies on simulating the feedbacks among atmospheric components and/or processes. Simulating hurricane Katrina using WRF, Rosenfeld et al. (2007b) reported a 25% reduction in the radius of hurricane force winds in response to warm rain suppression by sub-micron aerosols. By coupling a cloud microphysics module with WRF, Lynn et al. (2007) illustrates the suppression of precipitation by continental aerosols in the Sierra Nevada Mountains. Using a global-through-urban model, GATOR-GCMOM, over the Los Angeles basin, Jacobson et al. (2007) found that aerosol particles and their precursor gases reduce net downward surface total solar irradiance, near-surface temperature, and surface wind speed; increase RH, aerosol optical depth (AOD), and cloud optical thickness (COT), cloud fractions, cloud liquid water; and either increase or decrease precipitation depending on location and magnitude of precipitation intensity. Applying WRF/Chem over the eastern Texas in August 2000, Zhang (2008) showed that the presence of aerosols leads to a decrease in temperature by up to 0.18 °C at/near surface but an increase by 0.16 °C aloft in PBL (defined as the height from surface to ~2.9 km above the ground level (AGL)) at a site in the coastal area of the Galveston Bay, and Zhang et al. (in press) reported reduction of the domain-wide mean precipitation by 0.22–0.59 mm day^{-1} over the eastern Texas. In this work, WRF/Chem simulations are conducted at a horizontal grid spacing of 36 km for January and July 2001 over North America that covers the contiguous U.S. (CONUS), southern Canada, and northern Mexico to examine the importance of the aforementioned feedbacks. Seasonal variations in aerosol direct, semi-direct, and indirect feedbacks are analyzed and contrasted. Limitations and uncertainties in accurately representing such feedbacks to be addressed in future online-coupled model development and improvement are discussed.

2. Model setup and dataset for model evaluation

WRF/Chem version 2.2 released in March 2007 is applied for January and July 2001. The major physics options used include the Goddard shortwave radiation scheme, the Rapid Radiative Transfer Model (RRTM) longwave radiation scheme (Mlawer et al., 1997), the Fast-J photolysis rate scheme (Wild et al., 2000), the Yonsei University (YSU) PBL scheme (Hong et al., 2006), the National Center for Environmental Prediction, Oregon State University, Air Force, and Hydrologic Research Lab's (NOAH) land-surface module (Chen and Dudhia, 2001; Ek et al., 2003), the modified Purdue Lin microphysics module of Lin et al. (1983) and Chen and Sun (2002), and the Grell-Devenyi cumulus parameterization (Grell and Devenyi, 2002). The gas-phase chemistry is based on the Carbon-Bond Mechanism version Z (CBM-Z, Zaveri and Peters, 1999). The aerosol module is the Model for Simulating Aerosol Interactions and Chemistry (MOSAIC) (Zaveri et al., 2008). MOSAIC includes sulfate, methanesulfonate, nitrate, chloride, carbonate, ammonium, sodium, calcium, black carbon (BC), primary organic mass (OC), liquid water, and other inorganic mass (OIN) (e.g., trace metals, silica and other inert minerals). It simulates major aerosol processes (e.g., inorganic aerosol thermodynamic equilibrium, binary nucleation, coagulation, condensation, PM formation due to aqueous-phase chemistry, aerosol scavenged by cloud droplets, and dry and wet deposition) except for secondary organic aerosol formation. The particle size distribution is simulated in MOSAIC for eight size bins between 0.0390625 and 10 μm with six bins for $PM_{2.5}$ and two bins for $PM_{10\text{-}2.5}$. The bulk aqueous-phase chemistry of Fahey and Pandis (2001) is used, which includes 50 aqueous-phase species and 147 aqueous-phase chemical reactions (21 dissolution equilibria, 17 dissociation equilibria, and 109 kinetic reactions). The direct effect of aerosols on shortwave radiation is simulated based on Mie theory following the approach of Fast et al. (2006). The Goddard shortwave radiation scheme uses the prescribed fields of water vapor, CO_2, O_2, and O_3, and simulated concentrations of aerosols. The indirect effect of aerosols on cloud formation is accounted for through the effects of clouds on shortwave radiation, treatments of aerosol activation/resuspension, and prognostic CDNC based on activated aerosols, as described by Chapman et al. (2009). Aerosols are activated based on the parameterization of Abdul-Razzak and Ghan (2002), which determines the maximum supersaturation based on a Gaussian spectrum of updraft velocities and the fractions of activated aerosols to serve as CCN. The cloud microphysics is based on the modified Purdue Lin module from a one-moment module to a two-moment module to treat prognostic CDNC following Ghan et al. (1997) and simulate the second indirect effect (Skamarock et al., 2005). The autoconversion of cloud droplets to rain droplets is simulated using the parameterizations of Liu et al. (2005) that depends on cloud droplet number. The first indirect effect of aerosols is simulated by accounting for changes in shortwave radiation due to changes in droplet mean radius and COT resulted from changes in CDNC in the Goddard shortwave radiation scheme. More detailed chemistry, aerosol, and cloud treatments can be found in Fast et al. (2006), Gustafson et al. (2007), and Chapman et al. (2009).

The modeling domain covers the CONUS and a portion of southern Canada and northern Mexico with 148 × 112 horizontal grid cells. The horizontal resolution is 36 km. The vertical resolution includes 34 logarithmic structure layers from the surface to a fixed pressure of ~100 mb (or ~16 km AGL), with a finer resolution in the PBL (<~2.9 km, defined as the top of PBL height in this work). The first model layer height is set to be ~40 m AGL. The meteorological initial conditions (ICONs) and boundary conditions (BCONs) are generated using the National Centers for Environmental Prediction (NCEP) Final Analysis (FNL) reanalysis data. The

EPA's National Emissions Inventories (NEI) 2001 (also referred to as NEI 1999 Version 3) is used to generate a gridded anthropogenic emission inventory for gaseous and PM species. Chemical ICONs and BCONs for both gas and aerosol species are generated using the simulation results from a global chemistry model (i.e., GEOS-Chem) described in Park et al. (2003, 2004) and the GOES-Chem to CMAQ interface developed by Byun et al. (2004).

Since the Fast-J photolysis rate scheme computes photolytic rates based on predicted O_3, PM, and cloud profiles but the Goddard shortwave radiation scheme uses prescribed fields of O_3, predicted O_3 will not affect the shortwave radiation but will affect the photolysis rates and thus aerosol formation. To separate the effects of PM from those of gases on photolysis rates, two sets of model simulations are conducted for each month. In the baseline simulations, all meteorological and chemical processes of gas and PM as well as the feedbacks between meteorology and all chemical species including gases and aerosols are included. In the second simulation, all model treatments remain the same as the baseline simulation except that PM emissions and secondary PM formation are turned off, which essentially shuts off the feedbacks between meteorology and aerosols. Since both simulations use the same boundary conditions for PM which represent relatively clean conditions, the differences in model predictions between the two simulations are caused by additional PM resulted from primary PM emissions and gas-to-particle conversions under polluted environment; they provide an estimate of the aerosol feedbacks to shortwave radiation, PBL meteorology, and cloud formation. This approach is the same as that used in Jacobson et al. (2007) and similar to that used in Zanis (2009). The aerosol feedbacks are analyzed using domain-wide monthly-mean spatial distributions to minimize the chaotic nature of the relatively-short model simulations. Site-specific vertical profiles are also examined to study the aerosol feedback signals in several urban locations where the aerosol concentrations (thus the feedback signals) are high.

Simulated meteorology and species concentrations are evaluated using available observational data following the evaluation protocol of the U.S. EPA (2007) and Zhang et al. (2006). The domain-wide performance statistics are calculated in terms of mean bias (MB), the normalized mean bias (NMB), and the normalized mean gross error (NME), mean normalized bias (MNB), and the mean normalized error (MNE),as described in Zhang et al. (2006). Meteorological variables evaluated include temperature and relative humidity at 2-m (T2 and RH2) and in the PBL, wind speed and direction at 10-m (WSP10 and WDR10), and daily precipitation

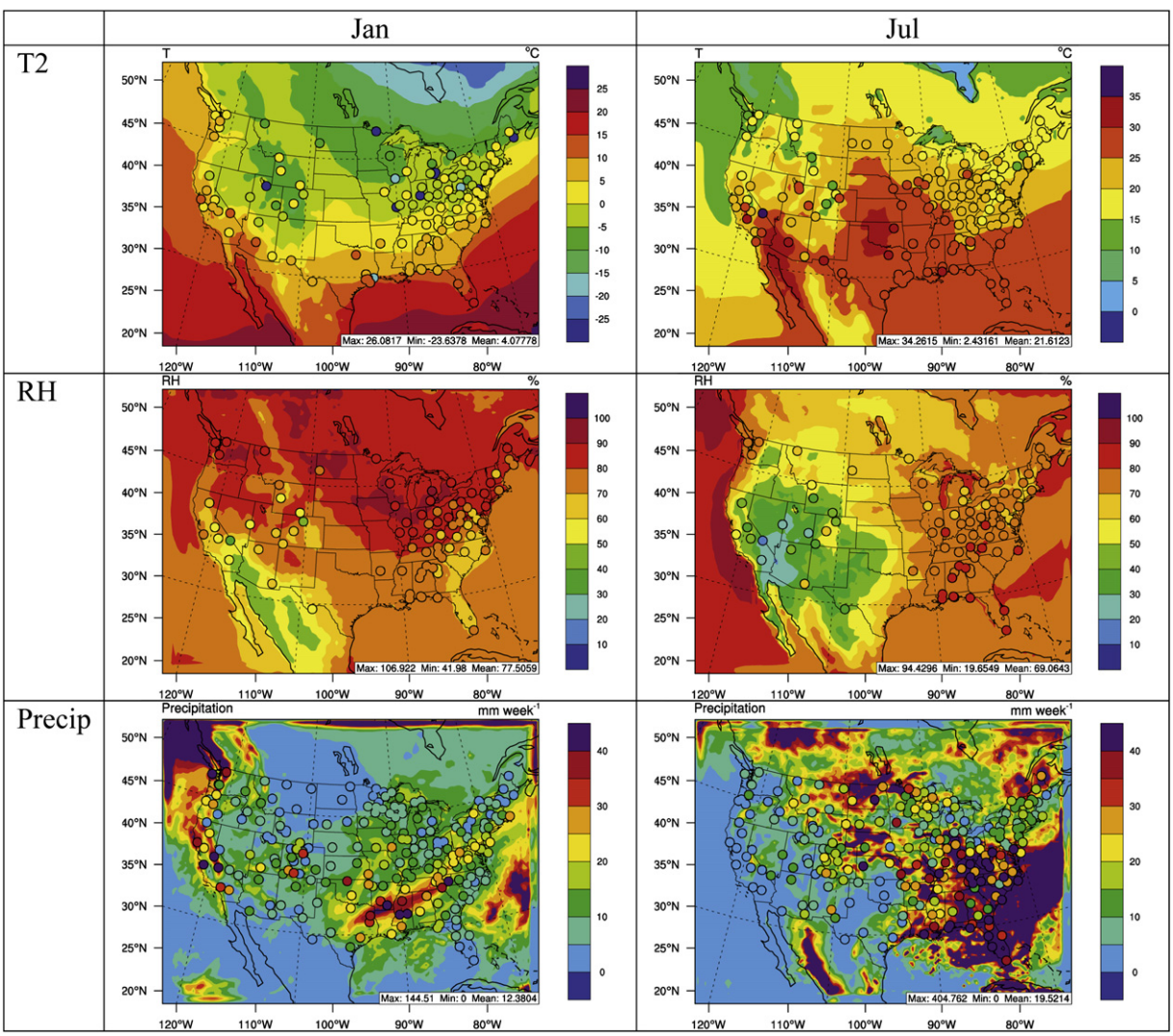

Fig. 1. Overlay of observed and simulated monthly-mean temperature and relative humidity at 2-m (T2 and RH2) and total daily precipitation (Precip). The observations for T2 are obtained from CASTNET, STN, and SEARCH, those for RH2 are obtained from STN and SEARCH, and those for Precip are obtained from NADP.

(Precip). The meteorological observational datasets include the Clean Air Status and Trends Network (CASTNET, http://www.epa.gov/castnet/), the Southeastern Aerosol Research and Characterization study (SEARCH, http://www.atmospheric-research.com/studies/SEARCH), the National Atmospheric Deposition Program (NADP, http://nadp.sws.uiuc.edu), and the National Center for Atmospheric Research (NCAR) Earth Observing laboratory atmospheric sounding data (http://weather.uwyo.edu/upperair/sounding.html). The maximum 1-h and 8-h average O_3 mixing ratios, the 24-h average mass concentrations of $PM_{2.5}$ and its composition (sulfate (SO_4^{2-}), nitrate (NO_3^-), ammonium (NH_4^+), black carbon (BC), organic carbon (OC)) are evaluated using the surface observations from one special field study (i.e., SEARCH) and four nationwide routine monitoring networks (i.e., CASTNET, the Aerometric Information Retrieval System -Air Quality System (AIRS-AQS, http://www.epa.gov/air/data/), the Interagency Monitoring of Protected Visual Environments (IMPROVE, http://vista.cira.colostate.edu/improve/), and the Speciation Trends Network (STN, http://www.epa.gov/air/data/)). The predicted total tropospheric column abundances of CO, NO_2, and O_3 and AODs are compared with derived quantities based on satellite products from the Measurements Of Pollution In The Troposphere (MOPITT, http://terra.nasa.gov/About/MOPITT/), the Global Ozone Monitoring Experiment (GOME, http://gcmd.gsfc.nasa.gov/records/GCMD_gov.noaa.class.GOME.html), the Total Ozone Mapping Spectrometer (TOMS)/the solar Backscattered Ultravoilet (SBUV) instrument (http://asd-www.larc.nasa.gov/TOR/TOR_Data_and_Images.html), and the Moderate Resolution Imaging Spectroradiometer (MODIS, http://ladsweb.nascom.nasa.gov), respectively.

3. Model evaluation

Fig. 1 shows the overlay plots of observed and simulated monthly-mean T2 and RH2 and total daily precipitation in Januray and July 2001. Table 1 summarizes the overall domain-wide model performance for both meteorological variables and chemical concentrations of species. The spatial distribution of T2 as well as areas with low temperatures (e.g., some areas in the Rocky

Table 1
The seasonal and annual performance statistics of WRF/Chem predictions in January and July 2001[a].

Variable[b]	Network	January					July				
		MB	NMB	NME	MNB	MNE	MB	NMB	NME	MNB	MNE
T2, °C	CASTNET	−0.73	−13.7	48.4	−19.0	167.0	0.07	0.3	11.3	1.3	12.5
	STN	0.06	0.8	35.9	−26.4	67.5	−1.53	−6.1	8.6	−6.1	8.9
	SEARCH	−0.22	−3.1	27.8	−12.1	24.1	−0.43	−1.5	7.9	−0.6	8.1
RH2, %	CASTNET	6.91	9.5	17.4	19.1	26.0	−0.36	−0.5	15.8	6.9	22.0
	SEARCH	−0.14	−0.2	13.9	4.3	16.4	−8.44	−10.5	14.1	−9.9	14.5
WSP10, m s^{-1}	CASTNET	2.16	89.6	102.1	294.2	303.1	1.54	78.1	96.1	272.1	282.9
	SEARCH	0.88	40.5	56.6	186.4	197.4	0.60	33.1	62.4	146.3	167.0
WDR10, degree	CASTNET	18.30	8.9	30.8	231.5	250.5	1.68	0.9	55.4	140.9	182.9
	SEARCH	−2.73	−1.3	26.5	1125	1149	5.41	2.9	36.9	277.0	303.4
Weekly total Precip, mm	NADP	2.84	21.2	65.7	301.6	328.2	6.66	32.3	98.0	532.3	576.0
Max 1-h O_3, ppb	CASTNET	−7.92	−22.6	27.6	−17.1	29.4	5.50	9.7	23.4	19.0	29.0
	AIRS-AQS	−4.33	−13.2	25.6	0.3	36.1	7.48	12.8	26.1	21.2	31.6
	SEARCH	−3.88	−10.8	20.2	−3.4	23.0	12.92	21.8	26.9	28.5	32.7
Max 8-h O_3, ppb	CASTNET	−7.06	−22.5	28.9	−16.0	32.7	7.40	14.5	25.2	21.7	29.5
	AIRS-AQS	−3.00	−10.8	28.3	14.4	49.5	9.24	18.1	28.2	27.1	35.2
	SEARCH	−3.02	−9.8	22.5	5.0	32.2	15.54	30.5	33.3	39.5	42.0
24-h avg. $PM_{2.5}$, μg m^{-3}	IMPROVE	1.34	32.2	70.9	95.5	126.0	0.63	8.5	57.6	12.0	55.0
	STN	−1.27	−6.7	63.9	63.8	113.0	2.84	21.5	58.8	30.9	66.3
	SEARCH	2.85	23.7	39.9	37.4	49.9	5.29	33.1	62.2	75.3	97.1
24-h avg. $SO4_{2.5}$, μg m^{-3}	CASTNET	−1.61	−64.4	65.1	−56.8	59.8	2.29	51.9	71.9	41.8	74.8
	IMPROVE	−0.58	−53.6	60.4	−40.3	58.7	0.83	34.0	81.5	32.2	81.0
	STN	−2.46	−60.7	71.3	17.2	115.2	0.64	12.7	61.1	19.5	68.7
	SEARCH	−0.22	−8.9	50.0	3.8	54.9	4.44	76.2	100.7	142.6	166.3
24-h avg. $NO3_{2.5}$, μg m^{-3}	CASTNET	0.12	5.3	51.2	166.4	198.9	0.95	275.60	340.3	774.0	810.1
	IMPROVE	0.0	0.0	77.3	126.1	193.9	0.49	160.4	235.7	240.4	310.7
	STN	−2.29	−46.2	68.0	265.3	350	0.73	42.9	164.4	311.6	364.7
	SEARCH	1.25	71.4	91.81	89.2	121.2	0.68	225.9	273.3	255.6	305.0
24-h avg. $NH4_{2.5}$, μg m^{-3}	CASTNET	−0.37	−26.6	35.5	−11.0	42.3	1.09	84.4	91.8	74.3	91.9
	IMPROVE	0.05	6.1	79.5	62.2	113.3	1.99	147.0	160.6	3084	3097
	STN	−1.86	−58.7	73.4	537.8	614.1	0.33	16.7	88.8	139.9	175.5
	SEARCH	0.22	16.0	43.4	25.1	51.4	1.83	108.6	125.7	195.6	215.2
24-h avg. $BC_{2.5}$, μg m^{-3}	IMPROVE	0.11	58.5	112.3	138.9	180.5	0.15	68.1	87.2	171.3	183.2
	SEARCH	−0.09	−7.0	61.8	52.5	87.4	−0.12	−14.3	51.7	37.0	77.6
24-h avg. $OM_{2.5}$, μg m^{-3}	IMPROVE	0.15	13.2	85.9	96.4	153.6	−0.63	−37.1	57.1	1.0	71.0
	SEARCH	0.53	10.0	55.8	37.6	64.7	−2.42	−49.4	57.2	−34.5	52.5
Tropospheric CO column[c, d]	MOPITT	0.15	0.8	8.6	2.73	9.98	4.55	34.4	35.0	47.33	47.80
Tropospheric NO_2 column[d]	GOME	0.90	33.9	84.4	51 191	51 203	0.66	47.1	61.1	11 291	11 297
Tropospheric O_3 column[d]	GOME	10.79	35.5	35.5	39.1	39.2	1.98	4.5	10.8	5.83	11.45
Aerosol optical depth[d]	MODIS	−0.07	−64.6	69.4	−56.8	66.8	0.01	3.7	93.2	17.74	105.1

[a] . The definitions of statistical measures are as follows (Zhang et al., 2006): MB $= 1/N\sum_{i=1}^{N}(M_i - O_i) = \overline{M} - \overline{O}$NMB $= [\sum_{i=1}^{N}(M_i - O_i)]/\sum_{i=1}^{N} O_i = (\overline{M}/\overline{O} - 1)$;NME $= [\sum_{i=1}^{N}|M_i - O_i|]/\sum_{i=1}^{N} O_i =$ MAGE$/\overline{O}$MNB $= 1/N\sum_{i=1}^{N}[(M_i - O_i)/O_i] = 1/N\sum_{i=1}^{N}(M_i/O_i - 1)$;MNE $= 1/N\sum_{i=1}^{N}[(|M_i - O_i|)/O_i]$ where $\overline{M} = (1/N)\sum_{i=1}^{N} M_i$, $\overline{O} = (1/N)\sum_{i=1}^{N} O_i$, M_i and O_i are values of model prediction and observation at time and location i, respectively. N is the number of samples (by time and/or location). The unit of MB is the same as that for each variable, and that for NMB, NME, MNB, and MNE is in %.

[b] . T2 – temperature at 2-m, RH2 – relative humidity at 2-m, WSP10-wind speed at 10-m, WDR10-wind direction at 10-m, Precip - Precipitation.

[c] . The statistics of column CO for summer is calculated based on the data in August. No data are available for June and July 2001.

[d] . The observational data are obtained for CO from MOPITT, ($\times 10^{18}$ molecules cm^{-2}), NO_2 from GOME ($\times 10^{14}$ molecules cm^{-2}), TOR from TOMS/SBUV and GOME (Dobson Unit), and AOD from MODIS.

mountain region and Middle Western states) in January and high temperatures (e.g., Texas, Oklahoma, and southern California and Arizona) in July are well reproduced. Cold biases in T2, however, occur over the western portions of Colorado and Wyoming, the eastern portions of Utah and Idaho, and a few sites in California in both months, as well as in Texas, and the southeastern and the northeastern U.S. in January. As shown in Table 1, cold biases are up to −0.73 °C in T2 (NMBs up to −13.7% and MNBs up to −26.4%) in January, and up to −1.53 °C (NMBs and MNBs up to −6.1%) in July. For comparison, MBs of −0.4 °C to −3.8 °C from applications of other meteorological models such as the Fifth-Generation NCAR/Penn State Mesoscale Model (MM5) have also been reported (e.g., Gilliam et al., 2006; Wu et al., 2008; Wang et al., 2009; Liu et al., 2010). Such cold biases are likely due to too cold soil initial temperatures in both months and inappropriate snow treatments in January (Liu et al., 2010), as well as limitations in the PBL scheme, land-surface model (LSM), and radiation schemes (Wang et al., 2009) in current meteorological models. Fig. 2 compares simulated vs. observed hourly T2 at two SEARCH sites: Jefferson Street (JST), Atlanta, GA (an urban site) and Yorkville, GA (a rural site). The model captures well the diurnal variations of T2 at JST in both months, although it overpredicts high and low temperatures at YRK during some time periods. Small underprediction in RH2 also occurs at the SEARCH sites in both months but small overprediction occurs at the CASTNET sites in January. The spatial distribution of RH2 in both months is generally captured except for some overpredictions in the Midwest in January and underpredictions in the southeastern U.S. in July. The model generally captures the diurnal variations of RH2 at JST and YRK in both months, despite underpredictions in hourly RH2 at both sites in both months, particularly in July.Fig. 3 compares simulated vertical profiles of temperature and relative humidity with atmospheric radiosonde observations recorded at 0000 and 1200 UTC July 2, 1001 between surface and 4000 m above ground level (AGL) at Peachtree City, approximately 40 km south-southwest of downtown Atlanta JST site, GA. While the model can capture the vertical profile of temperature relatively well, large deviations occur in vertical profiles of relative humidity.

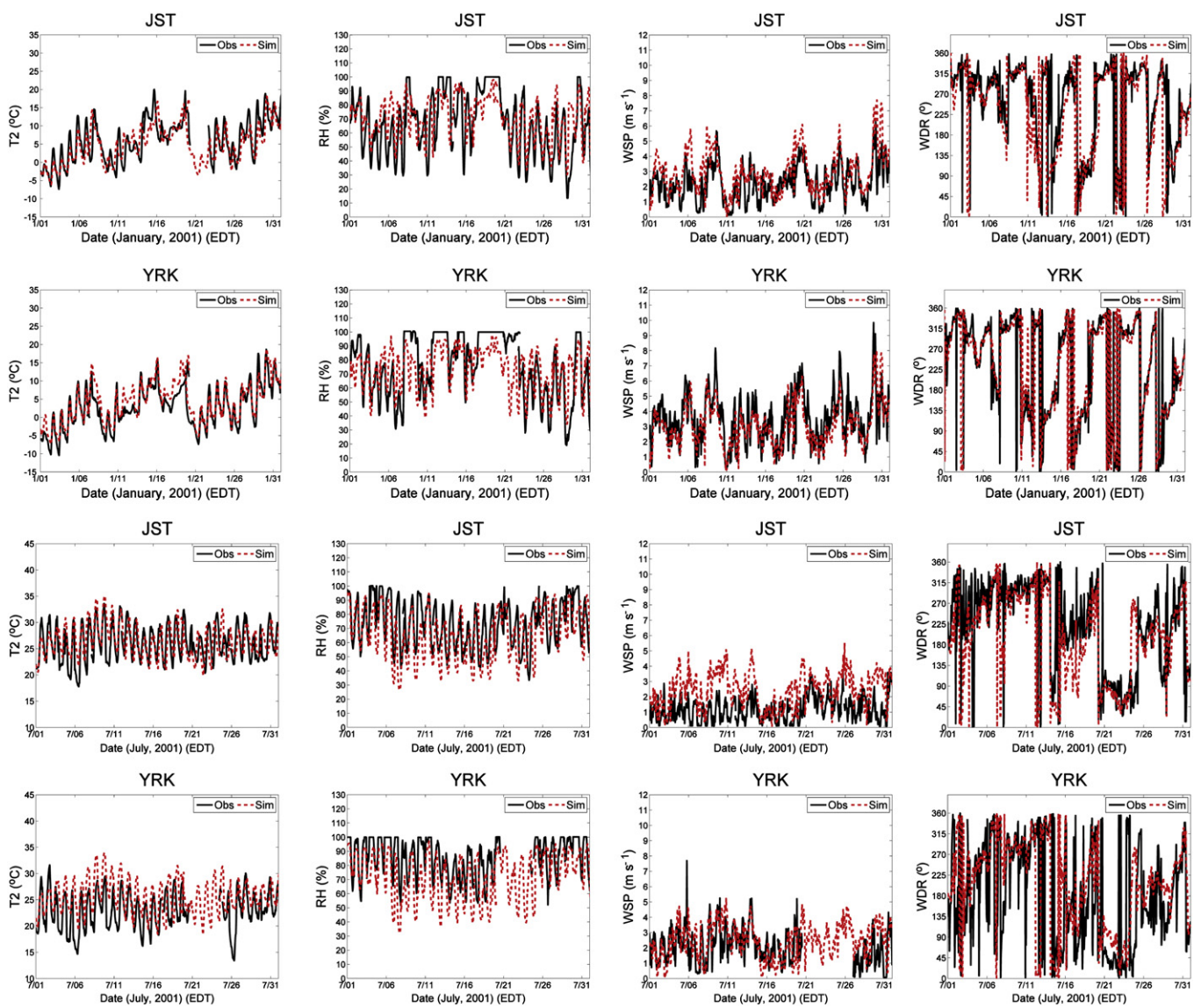

Fig. 2. The time series of the observed and simulated temperature and relative humidity (RH) at 2 m and wind speed (WSP) and wind direction (WDR) at 10-m during January (rows 1 and 2) and July (rows 3 and 4) 2001 at two SEARCH sites: Jefferson Street (JST), Atlanta, GA and Yorkville (YRK), GA.

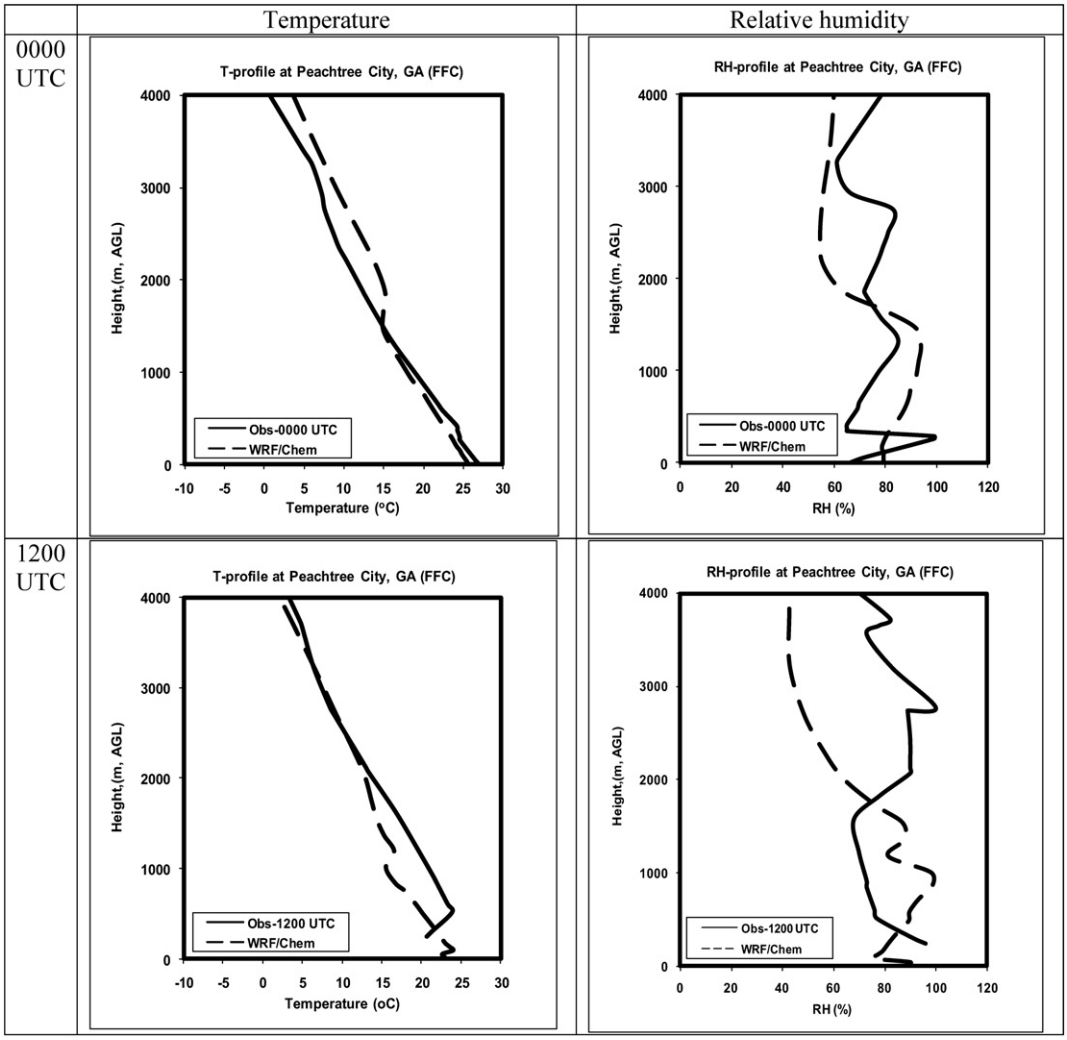

Fig. 3. Simulated vs. observed vertical profiles of temperature and relative humidity at Peachtree City, GA (site code: FFC) at 0000 and 1200 UTC between surface and 4000 m above ground level (AGL) on July 2, 2001. The observational data were obtained from the NCAR Earth Observing laboratory atmospheric sounding data (http://weather.uwyo.edu/upperair/sounding.html).

For WSP10 in January and July, moderate-to-large overpredictions occur with MBs of 2.16 and 1.54 m s^{-1} at the CASTNET sites and 0.88 and 0.6 m s^{-1} at the SEARCH sites, respectively. For WDR10 in January and July, MBs are 18.30 and 1.68° at the CASTNET sites and −2.73 and 5.41° at the SEARCH sites, respectively. The model generally reproduces well the hourly variations of WSP10 and WDR10 at both sites in January, WSP10 at YRK, and WDR10 at JST in July. It, however, overpredicts WSP10 at JST and gives relatively large deviations in WDR10 at YRK in July. The biases in domain-wide and hourly wind vectors are within the range of values reported but the MBs at the CASTNET sites in January are at the high end (e.g., Gilliam et al., 2006; Zhang et al., 2006; Wu et al., 2008), indicating model difficulties in capturing wind fields at a horizontal resolution of 36 km.

Weekly precipitations are moderately overpredicted in both months with NMBs of 21.2–32.3% and MNBs of 301.6–532.3%, which are comparable to those from MM5 applications reported earlier (e.g., Wu et al., 2008; Queen et al., 2008; Wang et al., 2009). Observed precipitations at some sites are very small, causing large MNBs values. The overpredictions occur in the northwestern and northeastern U.S. in January and the eastern U.S. in July. Such large positive biases in precipitation may be attributed to too frequent afternoon convective rainfall and/or an overestimation in the intensity of the rainfall typically simulated by meteorological models in summer (Olerud and Sims, 2004) and a bug in the Purdue Lin cloud microphysics that causes the overprediction of cloud ice, graupel, as well as surface rainfall (http://www.mmm.ucar.edu/wrf/users/wrfv3/known-prob.html) in WRF/Chem v3.0 and older.

Maximum 1-h and 8-h average O_3 mixing ratios are underpredicted with NMBs of −22.6% to −10.8% and −22.5% to −9.8% and MNBs of −17.1% to 0.3% and −16.0% to 14.4%, respectively, in January, due in part to the cold biases in T2 predictions. They are slightly-to-moderately overpredicted with NMBs of 9.7–30.5% and MNBs of 19.0–39.5%, respectively, in July. The overprediction in July is due in part to overestimated emissions of precursors such as NO_x emissions and in part to an artificial increase in the mass concentrations of gaseous precursors such as NO_x in WRF/Chem v2.2 that resets negative mass values around the sharp gradients near point source emissions and their downwind areas produced by the default non-positive definite advection scheme to zeros, artificially adding mass to the simulation (Chapman et al., 2009). For example, we found that the artificial increase in species mass concentrations due to the use of the non-positive definite scheme is up to about 10% over the eastern TX. The underpredictions in O_3 occur at some sites in the eastern U.S. in January and a few sites in California, central plains, and the eastern U.S. in July; the overpredictions in O_3

occur primarily in the eastern U.S. in July. As shown in Fig. 4, the model generally capture the hourly variations of the mixing ratios of O_3 at JST, YRK, North Birmingham (BHM) (an urban site), AL, and Centreville (CTR) (a rural site), AL in both months, although it tends to underpredict the peak O_3 values, particularly at YRK in January and overpredict them during some days at all sites in July.

The YSU scheme in WRF/Chem v2.2 arbitrarily sets an unrealistic value of 15-m for nocturnal PBL height, leading to a lower PBL height than what it should be at night (this problem has been corrected in WRF/Chem v. 3.0 (Hong et al., 2008)).The low PBL height may be a main factor contributing to the nighttime overpredictions of $PM_{2.5}$ at the IMPROVE and SEARCH sites that dominate daily predictions in both months (despite net underpredictions at a few sites in California and Washington D.C. area in January), consistent with the findings of Misenis and Zhang (2010). The cold bias in T2 favors the formation of $PM_{2.5}$, partially responsible for the positive biases at most sites in both months. The numerical artifact caused by the non-positive definite advection scheme may also contribute to the large overpredictions in $PM_{2.5}$ in July at the STN and SEARCH sites, which are located near the large point sources of the gaseous precursors of secondary $PM_{2.5}$ or their downwind areas. As shown in Table 1, the overpredictions in $PM_{2.5}$ may be attributed to the overestimations in the emissions of primary OM that dominate over underpredictions in secondary $PM_{2.5}$ such as sulfate, nitrate, and ammonium and other unknown inorganic aerosols in January, and overpredictions in secondary $PM_{2.5}$ (resulted from the above factors) that dominate over underpredictions in OM in July.Despite a dominant trend of overpredictions in $PM_{2.5}$ in both months, underpredictions occur at a few sites in California in both months and a few sites in central plains in July due largely to underestimations in wildfire emissions and incorrect temporal profiles of these emissions in those areas (Roy et al., 2007). The model reproduces well hourly variations and magnitudes of $PM_{2.5}$ at the four SEARCH sites during most days in January except a few days at JST (e.g., Jan. 11) and at BHM (e.g., Jan. 7). As shown in Fig. 4, larger discrepancies between simulated and observed hourly $PM_{2.5}$ concentrations occur at most sites in July, particularly during nighttime and early morning, due to the low nocturnal PBL height artificially set in the YSU scheme and the numerical artifact in the advection scheme mentioned previously.

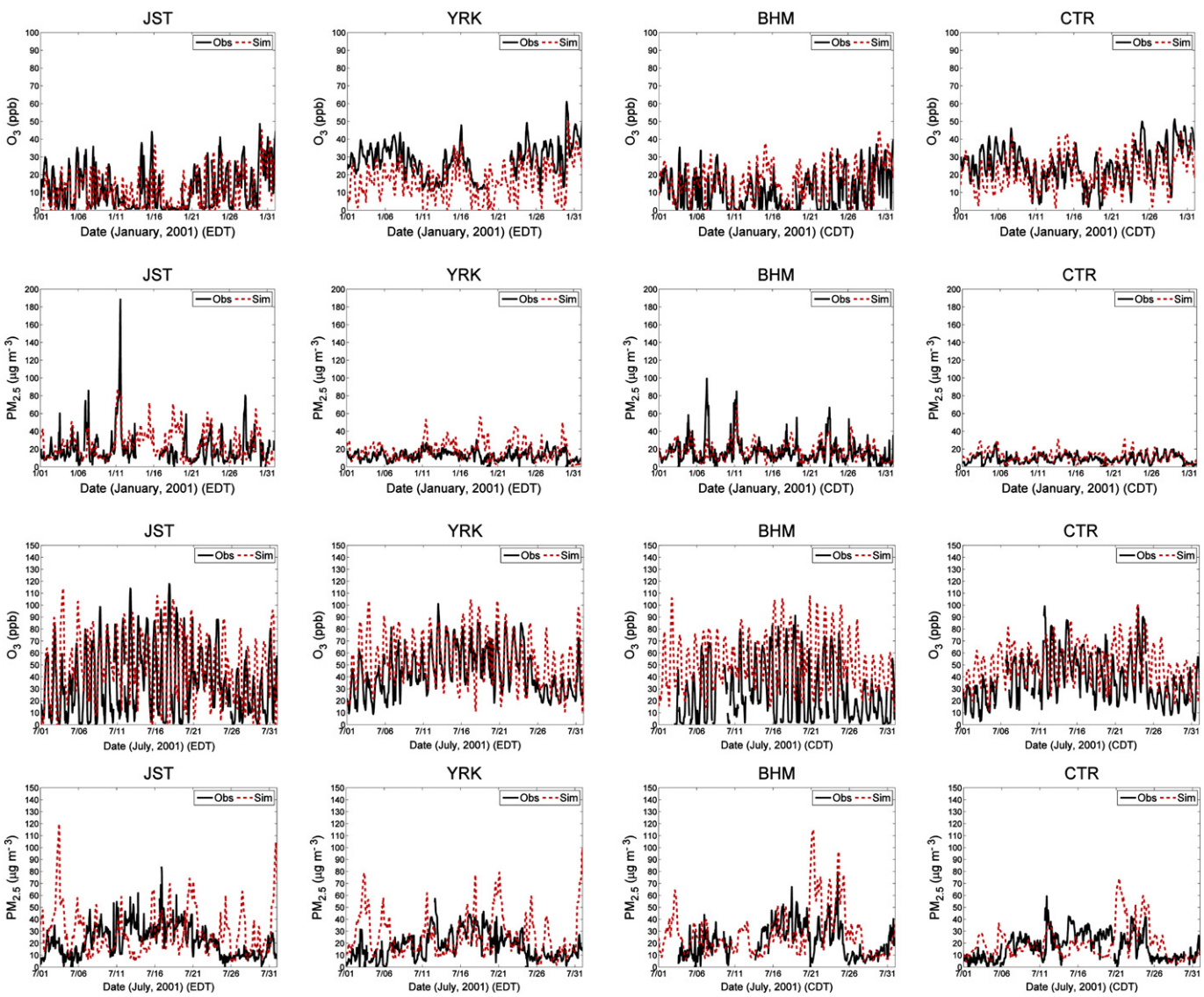

Fig. 4. The time series of the observed and simulated surface O_3 and $PM_{2.5}$ during January (rows 1 and 2) and July (rows 3 and 4), 2001 at four SEARCH sites: JST, YRK, North Birmingham (BHM), AL, and Centreville (CTR), AL.

The model generally overpredicts domain-wide column concentrations of CO and NO_2 and tropospheric O_3 residuals (TORs) in both months, with NMBs of 0.8–34.4%, 33.9–44.1%, and 4.5–35.5%, and MNBs of 2.7–47.3%, 11 291–51 191%, and 5.8–39.1%, respectively. Large MNBs for column concentrations of NO_2 are caused by very small observed values at some sites. The model gives a good agreement for domain-wide AODs in July but large underpredictions in AODs in January. As shown in Table 1, surface $PM_{2.5}$ concentrations are overpredicted at most sites in both months, which cannot explain different trends in AOD predictions in the two months. While AOD is underpredicted in most of the domain except for the southeastern U.S. in January, the overprediction in the

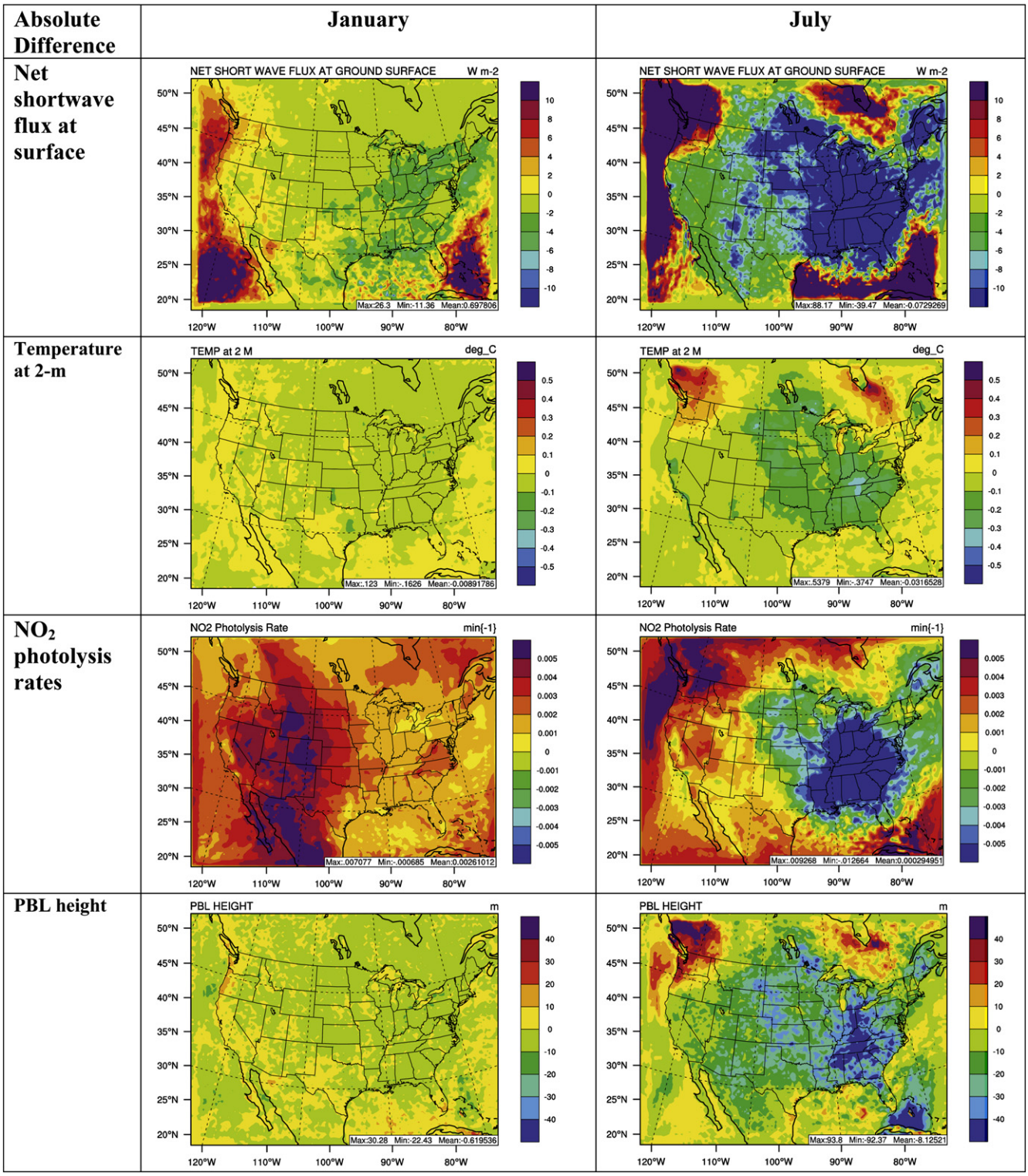

Fig. 5. Simulated direct and semi-direct effects of $PM_{2.5}$ on net shortwave flux at ground surface, temperature at 2-m, NO_2 photolysis rates, and PBL height during January and July, 2001.

eastern U.S. compensates the underprediction in the western U.S. in July, leading to an overall smaller bias in July than in January. The model biases in AOD predictions over different regions are due likely to overpredicted surface $PM_{2.5}$ in July, underpredicted $PM_{2.5}$ concentrations aloft over the whole domain in January and over the western U.S. in July, and other factors in both months including uncertainties in upper-layer boundary conditions of $PM_{2.5}$, inaccuracies in simulating aerosol size distribution and hydroscopic growth that propagate into the simulated AODs, as well as possible biases in the retrieval algorithm used in deriving MODIS AODs (Remer et al., 2005; Kaufman et al., 2005; Zhang et al., 2009a).

Despite model biases in simulating meteorological, chemical, and optical variables, the performance of WRF/Chem is generally consistent with most current air quality models. It is therefore suited for application for simulating aerosol feedbacks via direct and indirect effects.

4. Aerosol feedbacks

4.1. Direct and semi-direct feedbacks

Fig. 5 shows the direct effects of PM on net shortwave radiation and semi-direct effects on T2, NO_2 photolysis rate, and PBL height in terms of absolute differences caused by elevated aerosol concentrations under polluted environments. Aerosols affect radiation and temperature in several ways due to different radiative effects of different aerosol components (Jacobson, 1998). First, they can reduce incoming solar radiation via backscattering, therefore increasing the surface albedo and decreasing surface/near surface temperatures. This cooling effect occurs over most CONUS, where the domain-wide monthly-mean hourly shortwave radiation fluxes at surface reduce by up to 11.3 W m^{-2} (−9.1%) in January and up to 39.5 W m^{-2} in July (−16.1%) and T2 values reduce by up to 0.16 °C in January and 0.37 °C in July over most CONUS. The relative reductions in T2 are less than those in solar radiation over the eastern U.S., because near-surface temperatures are also affected by other factors such as soil moisture and soil temperature. PM decreases latent heat flux (by 5–10%) and soil temperatures, which increases soil moisture and water vapor, and thus T2. Such an increase compensates some decreases in T2, leading to less net decreases in T2.

Second, BC and UV-absorbing OC can absorb solar radiation and emit infrared radiation, offsetting the cooling effects caused by non-absorbing aerosol backscattering. This warming effect occurs over Pacific Northwest, southeastern Canada, and oceanic areas. Shortwave radiation increases over ocean and the western U.S. by up to 26.3 W m^{-2} (26.0%) in January and oceanic areas, Pacific

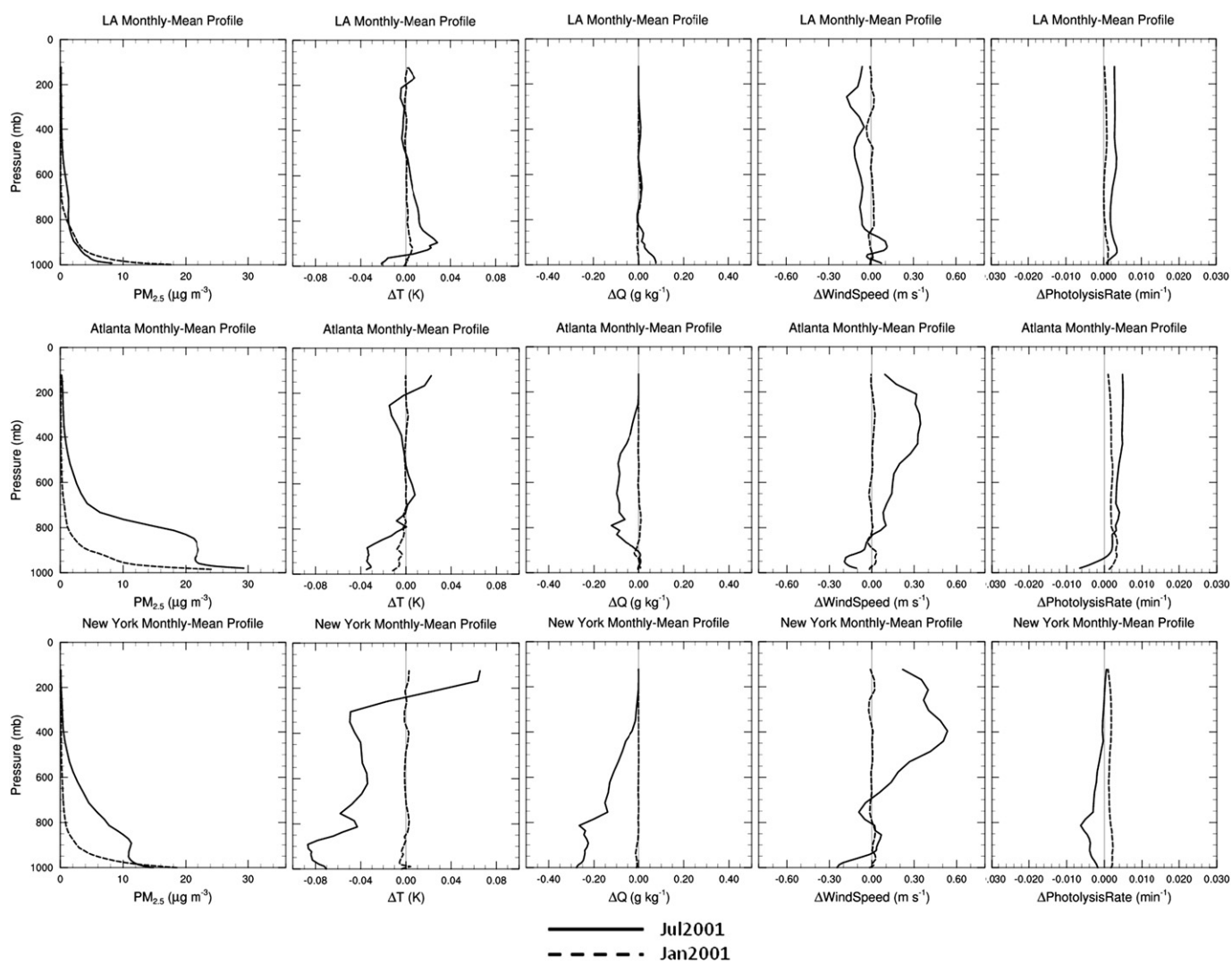

Fig. 6. Simulated monthly-mean vertical profiles of $PM_{2.5}$ concentrations and changes or temperature (ΔT), water vapor mixing ratio (ΔQ), wind speed (ΔWindSpeed), and photolysis rate (ΔPhotolysisRate) due to elevated aerosols in January and July 2001 at three sites: Los Angles (top), Atlanta (middle), and New York City (bottom).

Northwest, and southeastern Canada by up to 88.2 W m^{-2} (51%) in July. Such an increase is due to the fact that BC and UV-absorbing OC are abundant over those areas (e.g., they are directly emitted over land or advected into PBL and then subsequently transported to oceanic areas) and COTs decrease during both daytime and nighttime.

Third, aerosols can absorb and emit infrared radiation, also offsetting the cooling effect of backscattering during daytime. This warming effect is found over many areas in both months where longwave radiation slightly increases by up to 3.0 W m^{-2} (1.1%) in January and 10.3 W m^{-2} (3.1%) in July (Figure not shown). The simulated changes in shortwave and longwave fluxes as well as T2 over the South Coast Air Basin (SCAB) in California are generally consistent with the results of Jacobson et al. (2007) over the same region using a different model at a finer grid resolution of $0.045^\circ \times 0.05^\circ$ or $\sim$4.7 km $\times$ 5 km.

The changes in solar radiation and temperatures directly affect NO_2 photolysis rates, which in turn affect the formation of O_3 and $PM_{2.5}$. As a consequence of the relatively large reduction in shortwave radiation (i.e., actinic flux) and temperature over the central and eastern U.S. in July, NO_2 photolysis rates decrease by up to -0.012 min^{-1} (-8.2%) in this region. However, they increase by up to 0.0093 min^{-1} (6.9%) over the western U.S. in July and up to 0.007 min^{-1} (12.9%) over the entire domain in January, which do not reflect the reduction in solar radiation and temperatures. This is because the NO_2 photolysis rate also depends on other factors such as albedo and clouds (both height and fractions) and the net effect of aerosols on NO_2 photolysis depends on the dominant effect of different influential factors. For example, clouds can increase actinic fluxes within cloud layers but may change actinic fluxes below clouds in different ways. While low-level clouds may decrease actinic fluxes and temperatures below clouds due to their high albedo (Madronich, 1987), high-level clouds may increase actinic fluxes and temperatures below clouds due to their relatively-low albedos but strong absorptivity (Liou, 1992). Compared with the central and eastern U.S., the western U.S. in both months is characterized by higher albedos, solar radiation, NO_2 photolysis rates, wind speeds, and mixing heights but lower infrared radiation, latent heat fluxes, total cloud coverage (but higher low-level cloud fractions which lead to higher albedo), water vapor,

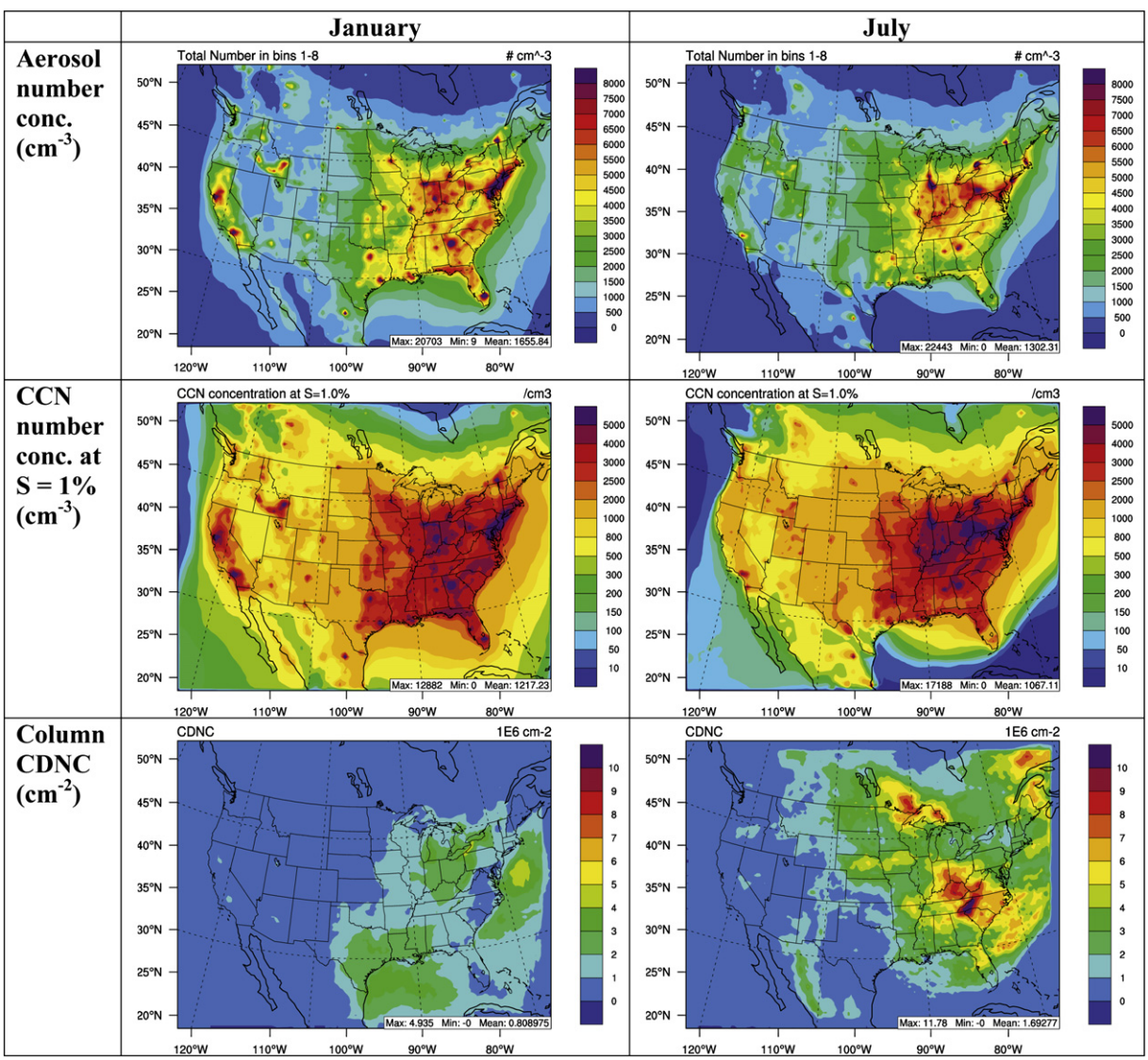

Fig. 7. Simulated concentrations of $PM_{2.5}$ number, cloud condensation nuclei (CCN), and cloud droplet number concentrations (CDNC) from the baseline simulations during January and July 2001.

precipitation, and soil moisture. In the presence of aerosols, shortwave radiation, latent heat, temperature, and soil temperature are reduced less or even increase (e.g., over Pacific Northwest), COT is either reduced or increased less (see Fig. 8), and longwave radiation increases (instead of decrease) in most areas in the western U.S. As a net result of these changes, NO_2 photolysis rates increase over the continental U.S. in January and the western U.S. in July. PBL height reduces by up to 22.4 m (−23.3%) in January and up to 92.4 m (−24%) in July, because of enhanced stability as a result of the warming caused by BC in the PBL and the cooling at surface resulted from reduced solar radiation. Reduced PBL height indicates a more stable PBL and can thus further exacerbate air pollution over areas where air pollution is already severe (so-called "chain effect").PBL heights increase by up to 30.3 m (16.4%) over the western U.S. and some oceanic areas in January and by up to 93.8 m (26.6%) over the Pacific Northwest, southeastern Canada, and some oceanic areas, due to increases in shortwave radiation and temperature at/near surface over those areas.

Fig. 6 shows the monthly-mean vertical profile of $PM_{2.5}$ and the changes in temperatures (T), water vapor mixing ratio (QV), wind speeds (WS), and NO_2 photolysis rates at three representative urban sites: Los Angles (LA) in the western U.S., Atlanta (AT) in the southeastern U.S., and New York City (NY) in the northeastern U.S. These changes reflect aerosol feedbacks to local meteorology. Monthly-mean T values in July reduce by up to 0.02, 0.035, and 0.07 °C at surface at LA, AT, and NY, respectively, due to the backscattering of solar radiation by aerosols, they increase at higher altitudes due to increased infrared radiation caused by absorbing aerosols such as black carbon between 600 and 950 mb at LA, 500–700 mb at AT, and 100–250 mb at NY. The changes of T in January are much smaller at all sites. Similar changes in vertical profiles of temperature are found in monthly-mean daytime (8 am–7 pm) and nighttime (8 pm–7 am) mean (Figures not shown). The simulated decreases at/near surface but increases in the PBL for T at LA are consistent with Ackerman (1977) and Jacobson (1998). The responses of QV to aerosol concentrations in January are very small at the three sites but differ significantly at all sites in July. They increase at/near surface and in the PBL at LA, remain nearly unchanged at/near surface but decrease through the remaining vertical domain up to 300 mb at AT, and decrease throughout the vertical domain up to 300 mb at NY. Such changes are caused by changes in several factors such as atmospheric radiation and temperature, cloud and precipitation, soil temperature and moisture. For example, water vapor will decrease when surface cooling occurs due to deceased evaporation, this may occur under the main aerosol plume such as that in NY and AT. Aerosols can affect patterns and magnitudes of local winds including sea-breezes. At AT and NY where aerosol concentrations are high, wind speeds in July decrease by up to 0.25 m s^{-1} at/near surfaces but increase by up to 0.52 m s^{-1} at higher altitudes, such changes further stabilize the atmosphere and enhance air pollution. At LA, changes in wind speeds are more complicated, because of a strong impact of sea-breezes on local wind fields, e.g., wind speed increases at surface and either decreases or increases in PBL. While the changes in photolysis rates in January remain nearly constant with a small increase at all sites, larger changes occur in July, with increases throughout the vertical domain at LA, decreases at/near surface but increases at higher altitudes at AT, and decreases throughout most of the vertical domain at NY. The largest reduction in NO_2 photolysis rates at surface occurs at AT due to the highest level of the surface aerosols that strongly absorb UV actinic fluxes.

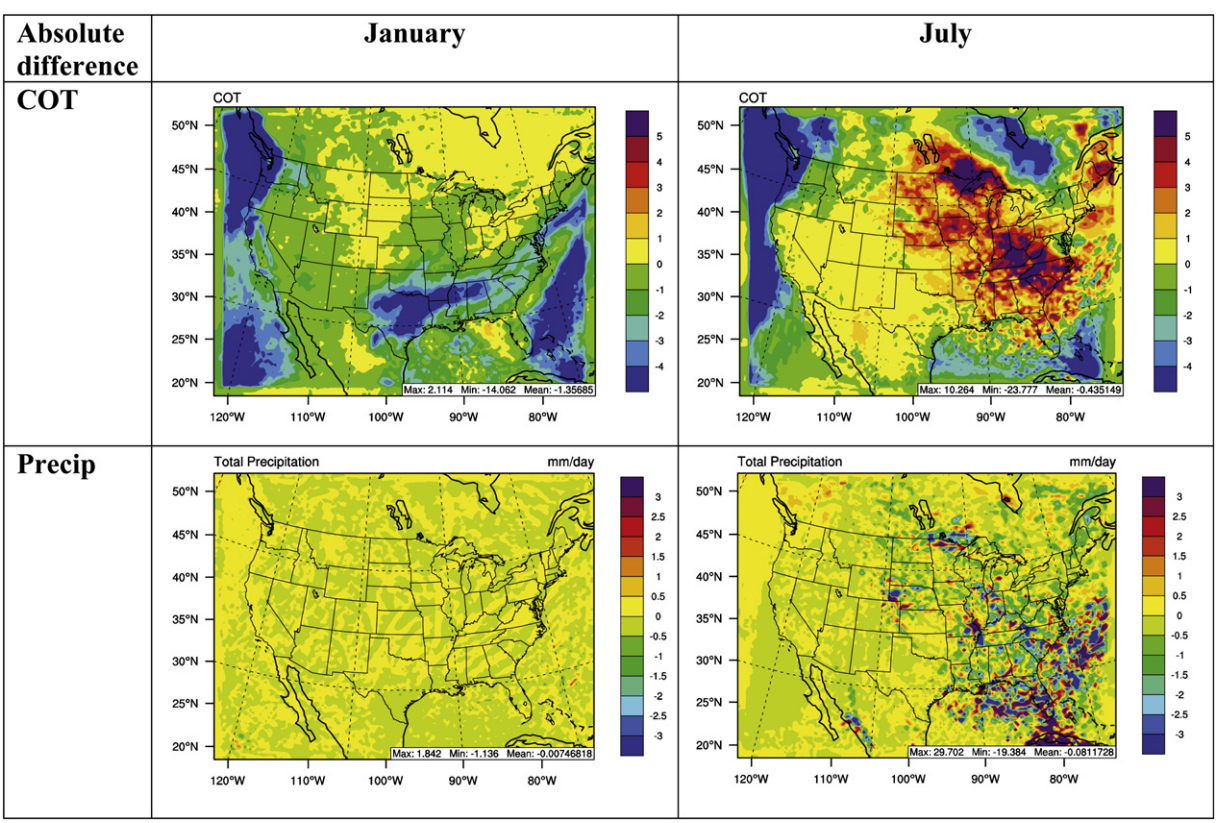

Fig. 8. Simulated changes in cloud optical thickness (COT) and precipitation (Precip) due to the presence of elevated aerosols in polluted environments during January and July 2001.

4.2. Indirect feedbacks

Fig. 7 shows PM number concentrations and CCN at a supersaturation (S) of 1.0% at surface, and the column-integrated CDNC from the met + gas + PM simulations. PM number concentrations are higher over the eastern U.S. than the western U.S. in both months, with domain-wide mean concentrations of 1655 cm^{-3} in January and 1302 cm^{-3} in July. CCN concentrations at $S = 1\%$ at surface are mostly in the range of 500–5000 cm^{-3} in both months over CONUS with higher values over most areas in July, particularly over the eastern U.S. A few exceptions occur in some areas such as California where higher CCN concentrations are predicted in January than in July due to higher aerosol number and mass concentrations resulted from higher primary PM emissions such as BC and primary OM during winter time. The predicted CCN concentrations over ocean are in the range of 10–500 cm^{-3}. For a qualitative comparison, the observed CCN concentrations range from 100 in remote marine regions to many thousands cm^{-3} in polluted urban areas (Seinfeld and Pandis, 2006). The total column CDNC concentrations are up to 4.9×10^6 cm^{-2} in January and up to 11.8×10^6 cm^{-2} in July, with higher values over regions where CCN concentrations and cloud fractions are high.

As a consequence of aerosol indirect effects on clouds and precipitations via acting as CCN, both COT and total daily

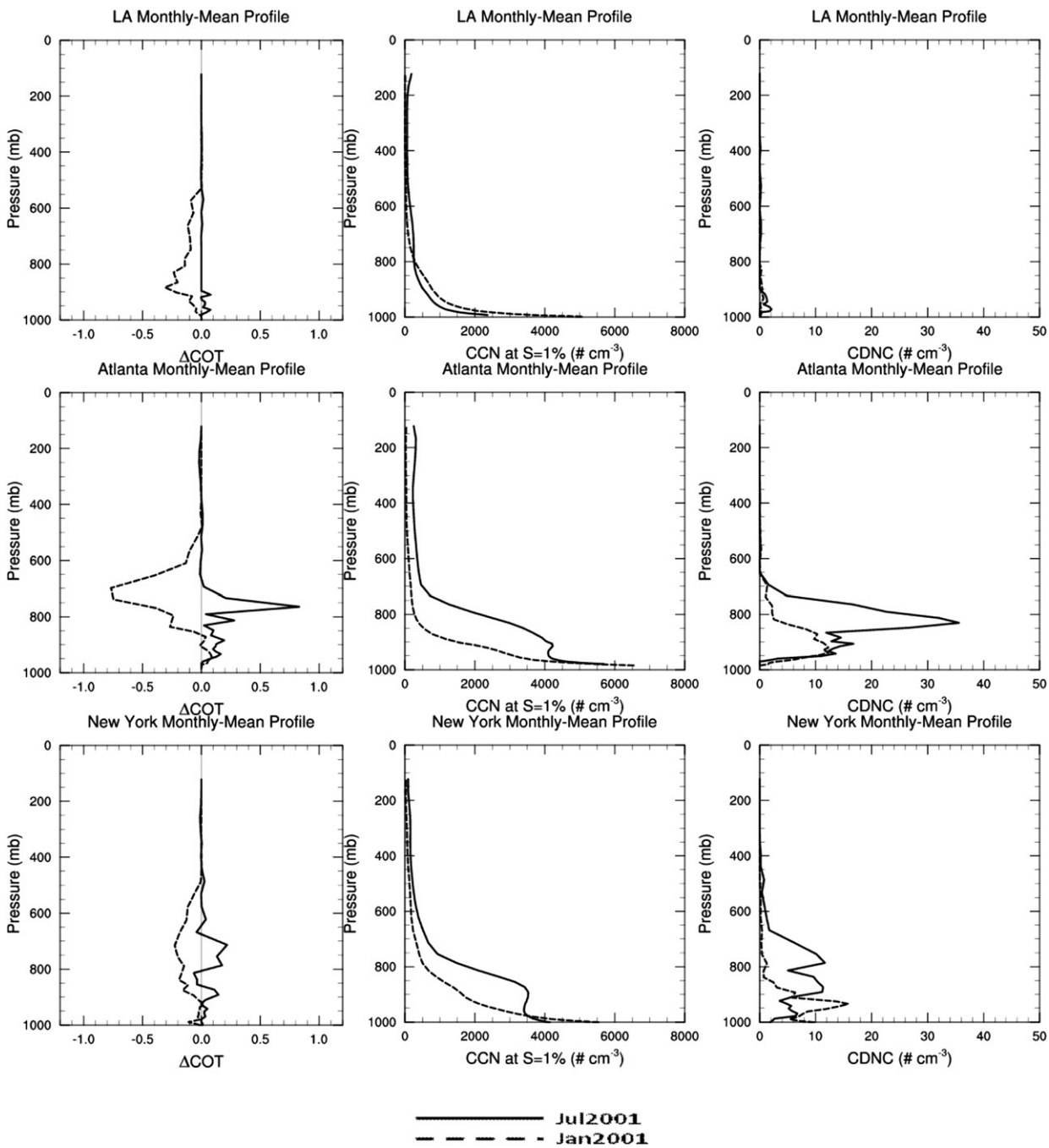

Fig. 9. Simulated monthly-mean vertical profiles of changes in COT (ΔCOT) due to the presence of elevated aerosols and absolute values of CCN and CDNC from the baseline simulations in January and July, 2001 at three sites: Los Angles (top), Atlanta (middle), and New York City (bottom).

precipitation are changed, as shown in Fig. 8. COT decreases in January but increases in July over most areas in CONUS. The decreases in some areas (e.g., oceanic areas, southern Canada, and Pacific Northwest) are greater than increases over remaining areas in July, leading to a net domain-wide decrease in COT. The effects of aerosols on precipitation in January are not pronounced (e.g., the changes are within 0.5 mm day^{-1} or $\pm$20%) because of their relatively small impact on cloud microphysics and autoconversion rates of cloud droplets to rain drops. Clouds involving precipitation are mostly ice clouds in January, but ice-nuclei (IN) is not simulated in the ice cloud microphysics module in WRF/Chem, so the impact of precipitation via IN cannot be simulated in this study. In July, such effects are more pronounced due to the presence of warm clouds. They reduce daily precipitation by up to 19.4 mm (or $\pm$100%) over most of the land areas due to the formation of small size CCNs, but they increase precipitation by a similar order of magnitude over Florida, some land areas, and many oceanic areas off the Atlantic coast due to the formation of large/giant CCN (e.g., activated sea-salt particles that can serve as CCN). Such results are consistent with those reported by other studies in which CCN is found to either depress or increase precipitation, depending on its size (e.g., Jauregui and Romales, 1996; Cerveny and Bailing, 1998; Givati and Rosenfeld, 2004, 2005; Rosenfeld et al., 2007a, 2008a; Jacobson et al., 2007). The reduction in precipitation may further reduce the wet removal rate of air pollutants, thus enhancing air pollution (Jacobson et al., 2007).

Fig. 9 shows the monthly-mean vertical profile of $PM_{2.5}$ and the changes in COT and simulated values of CCN at $S = 1\%$ and CDNC at LA, AT, and NY. COT in January decreases in the low atmosphere but increases at some heights due to greater abundance of clouds at those heights at all sites in July, in particular, at AT and NY where simulated aerosol concentrations are high. Because of higher aerosol concentrations in July in the PBL, the CCN concentrations at AT and NY are much higher in July than those in January, in contrast, the CCN concentrations at LA in both months are similar due to a similar amount of simulated aerosol concentrations, which reflects the model's incapability in reproducing observed PM concentrations and/or inaccuracies used in model inputs in July. CCN concentrations can reach up to 6500 cm^{-3} at individual sites. CDNCs in July are much higher at AT and NY due to higher CCN and cloud fractions, but much lower at LA due to lower cloud fractions. In January, lower CCN concentrations in the low atmosphere at AT and NY lead to lower CDNCs.

5. Conclusions

WRF/Chem is applied to study the chemistry–aerosol–cloud–radiation–climate feedbacks through aerosol direct, semi-direct, and indirect effects over the continental U.S. in January and July 2001. Despite the relative coarse horizontal grid resolution used in this study and some problems in WRF/Chem v2.2 model treatments, the model performance is overall consistent with current models, thus considered to be reasonably good in terms of its overall capability of reproducing observed meteorological variables, surface chemical concentrations, and column variables, although some improvements are expected with newer versions of WRF/Chem.

The model simulations show that aerosols can reduce incoming solar radiation via backscattering by up to 11.3 W m^{-2} ($-$9.1%) in January and up to 39.5 W m^{-2} ($-$16.1%) in July and 2-m temperatures by up to 0.16 °C in January and up to 0.37 °C in July over most of the CONUS on monthly average. The responses of NO_2 photolysis rates are either decreased by up to $-$8.2% due to reduced shortwave radiation and temperature over the central and eastern U.S. in July or increased by up to 6.9% over the western U.S. in July and up to 12.9% over the entire domain in January due to the effects of other factors such as longwave radiation, albedo and clouds, latent heat, and soil temperature. PBL height reduces by up to $-$23% to $-$24%, because of the warming caused by BC in the PBL and the cooling at surface resulted from reduced solar radiation. Such reductions can further stabilize PBL and thus exacerbate air pollution. Temperatures and wind speeds in July in big cities such as Atlanta and New York City reduce at/near surface but increase at higher altitudes. Similar to the effects of reduced PBL height, such changes further stabilize the atmosphere and enhance air pollution. Higher $PM_{2.5}$ concentrations generally lead to either decreases or smaller increases in the NO_2 photolysis rates throughout the vertical domain in July domain-wide and at individual sites.

For aerosol indirect effects, COT decreases in January but increases in July over most areas in the continental U.S. CCN concentrations at $S = 1\%$ at surface are mostly in the range of 500–5000 cm^{-3} over most land areas and 10–500 cm^{-3} over ocean in both months with higher values over most areas in July than in January, particularly over the eastern U.S. The total column CDNC concentrations are up to 4.9–11.8 $\times$ 10^6 cm^{-2}, with higher values over regions with high CCN concentrations and sufficient amounts of clouds. Aerosols can reduce daily precipitation by up to 19.4 mm day^{-1} (thus the wet removal rates) in July over most of the land areas due to the formation of small CCNs, but they can increase precipitation over some coastal and oceanic areas due to the formation of large/giant CCN. The total COTs decreases or increases at/near surface in both months, they remain decreasing or unchanged for upper layers in January but increase in July at some heights at individual sites. The vertical concentrations of CCN and CDNC domain-wide and at individual sites are proportional to those of $PM_{2.5}$, with much higher values in July than in January and at surface and in the PBL than above PBL.

While the above results demonstrate the importance of aerosol effects, the current study is subject to a number of limitations. Since $PM_{2.5}$ concentrations are overpredicted in the eastern U.S., the simulated aerosol feedbacks may represent the upper limit of the predictions with the feedback treatments available in WRF/Chem v2.2. Several known problems in the model treatments and the configurations available for aerosol feedback studies in WRF/Chem v2.2 will introduce inaccuracies and uncertainties in the model performance thus the magnitude of simulated aerosol feedbacks. For example, the low nocturnal PBL height in the YSU schemes and the non-positive advection scheme use in WRF/Chem v2.2 lead to large overpredictions in $PM_{2.5}$ concentrations near some source regions. The MOSAIC aerosol module does not simulate secondary organic aerosols and the Fast-J photolysis algorithm does not account for the feedbacks of all photochemically-active gases to photolysis. These incorrect or missing treatments will affect the accuracy of simulated gas and aerosol concentrations. Further, the Abdul-Razzak and Ghan (2002) activation parameterization in WRF/Chem neglects the size-dependence of the water vapor diffusivity coefficient and mass transfer coefficient, which may lead to an underestimation of CDNC. It does not treat the kinetic effect (i.e., mass transfer limitation) for larger particles for which the equilibrium Köhler theory may be inappropriate. Using a more advanced activation parameterization of Fountoukis and Nenes (2005), larger fractions of aerosols can be activated to serve as CCN (Wen et al., 2009), which would lead to stronger aerosol indirect effects. In addition, aerosol effects on cloud dynamic feedbacks associated with convective clouds and precipitation are currently not simulated in WRF/Chem, which may cause an underestimation in the aerosol indirect effects. Finally, the month-long simulation may still be too short to characterize the long-term variation trend. Nevertheless, this work represents one of the first studies on the chemistry–aerosol–cloud–radiation–climate

feedbacks through aerosol direct, semi-direct, and indirect effects over the continental U.S. and will thus provide a useful foundation upon which future improvements can be identified and focused. These results indicate potential importance of the aerosol feedbacks on a regional scale even at a time scale of a month, particularly over regions with high aerosol concentrations. The direct evaluation of simulated aerosol feedbacks with observations over CONUS in 2001 is, however, not possible due to a lack of data that were targeted for such an evaluation, although long-term meteorological/climatic and chemical measurements at some sites may be analyzed to provide qualitative evidence for such feedbacks (e.g., Zhang et al., 2009b) and to identify model deficiencies and areas of improvements. The uncertainties in simulated aerosol feedbacks and the lack of observational data for evaluation stress an urgent need for future field experiments to target for aerosol feedback studies and the accurate representations of such feedbacks in current atmospheric models to reduce uncertainties associated with climate change predictions.

Acknowledgements

This work was supported by the U.S. EPA-Science to Achieve Results (STAR) program (Grant # RD833376), the NSF Career Award No. Atm-0348819, the U.S. EPA/Office of Air Quality Planning & Standards via RTI International contract #4-321-0210288, and the Memorandum of Understanding between the U.S. Environmental Protection Agency (EPA). The authors thank Ken Schere, George Pouliot, and Warren Peters, U.S. EPA, for providing CMAQ model inputs that were used for WRF/Chem simulations in this study, Jack Fishman and John K. Creilson, NASA Langley Research Center, for providing Tropospheric Ozone Residual data, Xiao-Ming Hu, a former graduate student at NCSU, for his work on some earlier WRF/Chem simulations, and Ying Pan, Kai Wang, Yao-Sheng Chen, graduate students at NCSU, for post-processing some model results.

References

Abdul-Razzak, H., Ghan, S.J., 2002. A parameterization of aerosol activation. 3. Sectional representation. Journal of Geophysical Research 107 (D3). doi:10.1029/2001JD000483.

Ackerman, T.P., 1977. A model of the effect of aerosols on urban climates with particular applications to the Los Angeles basin. Journal of the Atmospheric Sciences 34, 531–546.

Bell, T.L., Rosenfeld, D., Kim, K.-M., Yoo, J.-M., Lee, M.-I., Hahnenberger, M., 2008. Midweek increase in U.S. summer rain and storm heights suggests air pollution invigorates rainstorms. Journal of Geophysical Research 113, D02209. doi:10.1029/2007JD008623.

Braham, R.R., Semonin, R.G., Auer, A.H., Changnon Jr., S.A., Hales, J.M., 1981. Summary of urban effects on clouds and rain. METROMEX: a review and summary. Meteorological monograph 40. American Meteor Society, 141–152.

Byun, D.W., Moon, N.K., Jacob, D., Park, R., 2004. Regional transport study of air pollutants with linked global tropospheric chemistry and regional air quality models. In: Presentation at the 2nd ICAP workshop, RTP, NC, October.

Cerveny, R.S., Bailing Jr., R.C., 1998. Weekly cycles of air pollutants, precipitation and tropical cyclones in the coastal NW Atlantic region. Nature 394, 561–563.

Chapman, E.G., Gustafson Jr., W.I., Easter, R.C., Barnard, J.C., Ghan, S.J., Pekour, M.S., Fast, J.D., 2009. Coupling aerosol-cloud-radiative processes in the WRF-Chem model: investigating the radiative impact of elevated point sources. Atmospheric Chemistry and Physics 9, 945–964.

Chen, F., Dudhia, J., 2001. Coupling an advanced land surface-hydrology model with the Penn State-NCAR MM5 modeling system. Part I: model implementation and sensitivity. Monthly Weather Review 129, 569–585.

Chen, S.-H., Sun, W.-Y., 2002. A one-dimensional time dependent cloud model. Journal of the Meteorological Society of Japan 80, 99–118.

Eagen, R.C., Hobbs, P.V., Radke, L.F., 1974. Particle emissions from a large Kraft paper mill and their effects on the microstructure of warm clouds. Journal of Applied Meteorology 13, 535–552.

Ek, M.B., Mitchell, K.B., Lin, Y., Rogers, B., Grunmann, P., Koren, V., Gayno, G., Tarpley, J.D., 2003. Implementation of NOAH land surface model advances in the National Centers for Environmental Prediction operational mesoscale Eta model. Journal of Geophysical Research 108 (D22), 8851.

Fahey, K.M., Pandis, S.N., 2001. Optimizing model performance: variable size resolution in cloud chemistry modeling. Atmospheric Environment 35, 4471–4478.

Fast, J.D., Gustafson Jr., W.I., Easter, R.C., Zaveri, R.A., Barnard, J.C., Chapman, E.G., Grell, G.A., 2006. Evolution of ozone, particulates, and aerosol direct forcing in an urban area using a new fully-coupled meteorology, chemistry, and aerosol model. Journal of Geophysical Research 111, D21305. doi:10.1029/2005JD006721.

Fountoukis, C., Nenes, A., 2005. Continued development of a cloud droplet formation parameterization for global climate models. Journal of Geophysical Research 110, D11212. doi:10.1029/2004JD005591.

Ghan, S.J., Leung, L.R., Easter, R.C., Abdul-Razzak, H., 1997. Prediction of cloud droplet number in a general circulation model. Journal of Geophysical Research 102 (D18), 21777–21794. doi:10.1029/97JD01810.

Gilliam, R.C., Hogrefe, C., Rao, S.T., 2006. New methods for evaluating meteorological models used in air quality applications. Atmospheric Environment 40, 5073–5086.

Givati, A., Rosenfeld, D., 2004. Quantifying precipitation suppression due to air pollution. Journal of Applied Meteorology 43, 1038–1056.

Givati, A., Rosenfeld, D., 2005. Separation between cloud-seeding and air-pollution effects. Journal of Applied Meteorology 44, 1298–1314.

Gustafson, W.I., Chapman, E.G., Ghan, S.J., Easter, R.C., Fast, J.D., 2007. Impact on modeled cloud characteristics due to simplified treatment of uniform cloud condensation nuclei during NEAQS 2004. Geophysical Research Letter 34 (L19809), L19809. doi:10.1029/2007GL0300321.

Grell, G.A., Devenyi, D., 2002. A generalized approach to parameterizing convection combining ensemble and data assimilation techniques. Geophysical Research Letter 29 (14) Article 1693.

Grell, G.A., Peckham, S.E., Schmitz, R., McKeen, S.A., Frost, G., Skamarock, W.C., Eder, B., 2005. Fully coupled "online" chemistry within the WRF model. Atmospheric Environment 39, 6957–6975.

Hong, S., Noh, Y., Dudhia, J., 2006. A new vertical diffusion package with an explicit treatment of entrainment processes. Monthly Weather Review 134, 2318–2341.

Hong, S.-Y., Kim, S.-W., Dudhia, J., Koo, M.-S., 2008. Stable boundary layer mixing in a vertical diffusion package, presented at the 9th Annual WRF workshop, June 23–27, Boulder, Colorado.

IPCC, 2007. Climate change 2007: the physical science basis. In: Solomon, S., Qin, D., Manning, M. (Eds.), Contribution of Working Group I to the Fourth Assessment Report of the Intergovernmental Panel on Climate Change.

Jacob, D.J., Winner, D.A., 2009. Effect of climate change on air quality. Atmospheric Environment 43, 51–63.

Jacobson, M.Z., 1998. Studying the effects of aerosols on vertical photolysis rate coefficient and temperature profiles over an urban airshed. Journal of Geophysical Research 103, 10,593–10,604.

Jacobson, M.Z., 2002. Atmospheric Pollution: History, Sciences and Regulation. Cambridge University Press, New York, ISBN 0521010446, 399 pp.

Jacobson, M.Z., Kaufmann, Y.J., Rudich, Y., 2007. Examining feedbacks of aerosols to urban climate with a model that treats 3-D clouds with aerosol inclusions. Journal of Geophysical Research 112, D24205. doi:10.1029/2007JD008922.

Jauregui, E., Romales, E., 1996. Urban effects on convective precipitation in Mexico city. Atmospheric Environment 30, 3383–3389.

Kaufman, Y.J., Fraser, R.S., 1997. The effect of smoke particles on clouds and climate forcing. Science, Washington, DC 277 (5332), 1636–1638.

Kaufman, Y.J., Koren, I., Remer, L.A., Tanre, D., Ginoux, P., Fan, S., 2005. Dust transport and deposition observed from the Terra-Moderate Resolution Imaging Spectroradiometer (MODIS) spacecraft over the Atlantic Ocean. Journal of Geophysical Research 110, D10S12. doi:10.1029/2003JD004436.

Klüser, L., Rosenfeld, D., Macke, A., Holzer-Popp, T., 2008. Observations of convective clouds generated by solar heating of dark smoke plumes. Atmospheric Chemistry and Physics 8, 2833–2840.

Koren, I., Kaufman, Y.J., Rosenfeld, D., Remer, L.A., Rudich, Y., 2005. Aerosol invigoration and restructuring of Atlantic convective clouds. Geophysical Research Letter 32, L14828. doi:10.1029/2005GL023187.

Lau, K.-M., Kim, K.-M., 2006. Observational relationships between aerosol and Asian monsoon rainfall, and circulation. Geophysical Research Letter 33, L21810. doi:10.1029/2006GL027546.

Lau, K.M., Kim, M.K., Kim, K.M., 2006. Asian monsoon anomalies induced by aerosol direct effects. Climate Dynamics 26, 855–864. doi:10.1007/s00382-006-0114-z.

Levin, Z., Ganor, E., Gladstein, V., 1996. The effects of desert particles coated with sulfate on rain formation in the eastern Mediterranean. Journal of Applied Meteorology 35, 1511–1523.

Levin, Z., Teller, A., Ganor, E., Yin, Y., 2005. On the interactions of mineral dust, sea salt particles and clouds – a measurement and modeling study from the MEIDEX campaign. Journal of Geophysical Research 110, D20202. doi:10.1029/2005JD005810.

Levin, Z., Brenguier, J.-L., 2009. Effects of pollution and biomass aerosols on clouds and precipitation: observational studies, Chapter 6. In: Levin, Z., Cotton, W.R. (Eds.), Aerosol Pollution Impact on Precipitation: a Scientific Review. Springer, ISBN 978-1-4020-8689-2.

Lin, Y.-L., Farley, R.D., Orville, H.D., 1983. Bulk parameterization of the snow field in a cloud model. Journal of Climate and Applied Meteorology 22, 1065–1092.

Liou, K.-N., 1992. Radiation and Cloud Processes in the Atmosphere. Oxford Univ. Press, New York.

Liu, Y., Daum, P.H., McGraw, R.L., 2005. Size truncation effect, threshold behavior, and a new type of autoconversion parameterization. Geophysical Research Letter 32, L11811. doi:10.1029/2005GL022636.

Liu, X.-H., Zhang, Y., Olsen, K., Wang, W.-X., Do, B., Bridgers, G., 2010. Responses of future air quality to emission controls over North Carolina, part I: model evaluation for current-year simulations. Atmospheric Environment 44 (23), 2443–2456.

Lynn, B., Khain, A., Rosenfeld, D., Woodley, W.L., 2007. Effects of aerosols on precipitation from orographic clouds. Journal of Geophysical Research 112, D10225. doi:10.1029/2006JD007537.

Madronich, S., 1987. Photodissociation in the atmosphere 1. Actinic flux and the effects of ground reflection and clouds. Journal of Geophysical Research 92, 9740–9752.

Mlawer, E.J., Taubman, S.J., Brown, P.D., Iacono, M.J., Clough, S.A., 1997. Radiative transfer for inhomogeneous atmospheres: RRTM, a validated correlated-k model for the longwave. Journal of Geophysical Research 102 (D14), 16,663–16,682.

Miller, R.L., Tegen, I., Perlwitz, J., 2004. Surface radiative forcing by soil dust aerosols and the hydrologic cycle. Journal of Geophysical Research 109, D04203. doi:10.1029/2003JD004085.

Misenis, C., Zhang, Y., 2010. An examination of WRF/Chem: physical parameterizations, nesting options, and grid resolutions. Atmospheric Research 97, 315–334.

Olerud, D., Sims, A., 2004. MM5 2002 modeling in support of VISTAS (Visibility Improvement – State and Tribal Association of the Southeast). http://www.baronams.com/projects/VISTAS/reports/VISTAS_TASK3f_final.pdf.

Park, R.J., Jacob, D.J., Chin, M., Martin, R.V., 2003. Sources of carbonaceous aerosols over the United States and implications for natural visibility. Journal of Geophysical Research 108 (D12), 4355. doi:10.1029/2002JD003190.

Park, R.J., Jacob, D.J., Field, B.D., Yantosca, R.M., Chin, M., 2004. Natural and transboundary pollution influences on sulfate-nitrate-ammonium aerosols in the United States: implications for policy. Journal of Geophysical Research 109, D15204. doi:10.1029/2003JD004473.

Queen, A., Zhang, Y., Gilliam, R., Pleim, J., 2008. Examining the sensitivity of MM5-CMAQ predictions to explicit microphysics schemes and horizontal grid resolutions, part I—database, evaluation protocol, and precipitation predictions. Atmospheric Environment 42, 3842–3855.

Ramanathan, V., Carmichael, G.R., 2008. Global and regional climate changes due to black carbon. Nature Geosciences 1, April.

Remer, L.A., Kaufman, Y.J., Tanré, D., Mattoo, S., Chu, D.A., Martins, J.V., Li, R.-R., Ichoku, C., Levy, R.C., Kleidman, R.G., Eck, T.F., Vermote, E., Holben, B.N., 2005. The MODIS aerosol algorithm. Products and validation. Journal of the Atmospheric Sciences 62, 947–973.

Rosenfeld, D., Lensky, I.M., 1998. Spaceborne sensed insights into precipitation formation processes in continental and maritime clouds. Bulletin of the American Meteorological Society 79, 2457–2476.

Rosenfeld, D., Woodley, W.L., 1999. Satellite-inferred impact of aerosols on the microstructure of Thai convective clouds. In: Proceedings, Seven WMO Scientific Conference on Weather Modification, Chiang Mai, Thailand, 17–22 February 1999, 17–20.

Rosenfeld, D., 1999. TRMM observed first direct evidence of smoke from forest fires inhibiting rainfall. Geophysical Research Letter 26 (20), 3105–3108.

Rosenfeld, D., 2006. Aerosol-cloud interactions control of earth radiation and latent heat release budgets. Space Science Review 125, 149–157.

Rosenfeld, D., Dai, J., Yu, X., Yao, Z., Xu, X., Yang, X., Du, C., 2007a. Inverse relations between amounts of air pollution and orographic precipitation. Science 315.

Rosenfeld, D., Khain, A., Lynn, B., Woodley, W.L., 2007b. Simulation of hurricane response to suppression of warm rain by sub-micron aerosols. Atmospheric Chemistry and Physics 7, 3411–3424.

Rosenfeld, D., Woodley, W.L., Axisa, D., Freud, E., Hudson, J.G., Givati, A., 2008a. Aircraft measurements of the impacts of pollution aerosols on clouds and precipitation over the Sierra Nevada. Journal of Geophysical Research 113, D15203. doi:10.1029/2007JD009544.

Rosenfeld, D., Lohmann, U., Raga, G.B., O'Dowd, C.D., Kulmala, M., Fuzzi, S., Reissell, A., Andreae, M.O., 2008b. Flood or drought: how do aerosols affect precipitation? Science 321, 1309–1313.

Roy, B., Pouliot, G.A., Gilliland, A., Pierce, T., Howard, S., Bhave, P.V., Benjey, W., 2007. Refining fire emissions for air quality modeling with remotely sensed fire counts: a wildfire case study. Atmospheric Environment 41, 655–665.

Rudich, Y., Sagi, A., Rosenfeld, D., 2003. Influence of the Kuwait oil fires plume (1991) on the microphysical development of clouds. Journal of Geophysical Research 108 (D15), 4478. doi:10.1029/2003JD003472.

Seinfeld, J.H., Pandis, S., 2006. Atmospheric Chemistry and Physics: from Air Pollution to Climate Change. John Wiley & Sons, Inc, ISBN 978-0-471-72018-8.

Skamarock, W.C., Klemp, J.B., Dudhia, J., Gill, D.O., Barker, D.M., Wang, W., Powers, J. G., 2005. A Description of the Advanced Research WRF Version 2, NCAR Technical Note, NCAR/TN-468+STR. http://wrf-model.org/wrfadmin/publications.php, 88 pp.

U.S. EPA, 2007. Guidance on the Use of Models and Other Analyses for Demonstrating Attainment of Air Quality Goals for Ozone, $PM_{2.5}$, and Regional Haze, Final Report. EPA-454/B-07–002, April, 2007. the U.S. Environmental Protection Agency, Office of Air and Radiation/Office of Air Quality Planning and Standards, Research Triangle Park, NC 27711.

Wang, K., Zhang, Y., Jang, C.J., Phillips, S., Wang, B.-Y., 2009. Modeling study of Intercontinental air pollution transport over the Trans-Pacific region in 2001 using the community multiscale air quality (CMAQ) modeling system. Journal of Geophysical Research 114, D04307. doi:10.1029/2008JD010807.

Warner, J., 1968. A reduction in rainfall associated with smoke from sugar cane fires – an inadvertent weather modification? Journal of Applied Meteorology 7, 247–251.

Wen, X.-Y., Pan, Y., Zhang, Y., Nenes, A., Ghan, S.J., Easter, R.C., 2009. CCN predictions from global WRF/Chem: sensitivity to activation parameterizations and aerosol modules, oral presentation at the 11th Conference on Atmospheric Chemistry/the 89th AMS Annual Meeting, Phoenix, AZ, January 11–15.

Wild, O., Zhu, X., Prather, M.J., 2000. Fast-J: accurate simulation of in- and below cloud photolysis in tropospheric chemical models. Journal of Atmospheric Chemistry 37, 245–282.

Wu, S.-Y., Krishnan, S., Zhang, Y., Aneja, V., 2008. Modeling atmospheric transport and fate of ammonia in North Carolina, part I. Evaluation of meteorological and chemical predictions. Atmospheric Environment 42, 3419–3436.

Zanis, P., 2009. A study on the direct effect of anthropogenic aerosols on near surface air temperature over Southeastern Europe during summer 2000 based on regional climate modeling. Annales Geophysicae 27, 3977–3988.

Zaveri, R.A., Peters, L.K., 1999. A new lumped structure photochemical mechanism for large-scale applications. Journal of Geophysical Research 104, 30,387–30,415.

Zaveri, R.A., Easter, R.C., Fast, J.D., Peters, L.K., 2008. Model for simulating aerosol interactions and chemistry (MOSAIC). Journal of Geophysical Research 113, D13204. doi:10.1029/2007jd008782.

Zhang, R., Li, G., Fan, J., Wu, D.L., Molina, M.J., 2007. Intensification of Pacific storm track linked to Asian pollution. Proceedings of the National Academy of Sciences U S A 104, 5295–5299.

Zhang, Y., Liu, P., Pun, B., Seigneur, C., 2006. A comprehensive performance evaluation of MM5-CMAQ for the summer 1999 southern oxidants study episode, part-I. Evaluation protocols, databases and meteorological predictions. Atmospheric Environment 40, 4825–4838.

Zhang, Y., 2008. Online coupled meteorology and chemistry models: history, current status, and outlook. Atmospheric Chemistry and Physics 8, 2895–2932.

Zhang, Y., Vijayaraghavan, K., Wen, X.-Y., Snell, H.E., Jacobson, M.Z., 2009a. Probing into regional O_3 and PM pollution in the U.S., Part I. A 1-year CMAQ simulation and evaluation using surface and satellite data. Journal of Geophysical Research 114, D22304. doi:10.1029/2009JD011898.

Zhang, Y., Pan, Y., Wen, X.-Y., Dong, X.-Y., Karamchandani, P., Streets, D.G., Skamarock, W.C., Grell, G.A., 2009b. Simulating climate-air quality interactions using global-through-urban WRF/Chem, oral presentation at the 11th Conference on Atmospheric Chemistry/the 89th AMS Annual Meeting, Phoenix, AZ, January 11–15.

Zhang, Y., Pan, Y., Wang, K., Fast, J.D., Grell, G.A. Incorporation of MADRID into WRF/Chem and initial application to the TexAQS-2000 Episode. Journal of Geophysical research, in press.